



## Cultural-Centric Online English Teaching with Artificial Intelligence Technology and Decision Support System

Jing Chen<sup>1</sup>  and Jindan Yang<sup>2\*</sup> 

<sup>1</sup>Department of International Education and Exchange, Tangshan Vocational and Technical College, Tangshan, Hebei 063004, China

[Eva197802@126.com](mailto:Eva197802@126.com)

<sup>2</sup> School of Foreign Studies, Yanshan University, Qinhuangdao, Hebei 066004, China

[yjindan@163.com](mailto:yjindan@163.com)

Corresponding author: Jindan Yang, [yjindan@163.com](mailto:yjindan@163.com)

**Abstract.** To improve the effectiveness of online English teaching, this paper combines artificial intelligence technology and a decision support system to enhance the English online teaching mode and the intelligence level of English online teaching. Moreover, this paper designs a structured three-layer college English online teaching decision support system architecture, builds a fully distributed microcavity array fiber demodulation optical path, and analyzes how to perform the range domain demodulation and reflection spectrum demodulation of the microcavity array. Then, this paper compensates for the nonlinear effect of the scanning laser to improve the feature recognition effect of online teaching. The research shows that the online English teaching mode based on artificial intelligence technology and the decision support system proposed in this paper can effectively improve the effect of online English teaching.

**Keywords:** artificial intelligence technology; decision support; online English; teaching; Cultural-Centric.

**DOI:** <https://doi.org/10.14733/cadaps.2024.S20.177-191>

### 1 INTRODUCTION

The dual-track teaching mode of online theory and project practice is constructed by adopting online theoretical teaching, virtual training projects, and real-world practice, providing students with a comprehensive communication environment, learning environment, design environment, and production environment. Currently, the design project courses based on network teaching are single online courses and online and offline hybrid courses [4]. Literature [7] tried a blended design course teaching mode from different angles, combining traditional face-to-face teaching with online learning, using the form of online learning to preview basic knowledge or extend

content, providing students with a relatively accessible learning space respecting the individualized development of students and the characteristics of autonomous learning. Literature [8] tries to build a highly interactive online and offline co-creation workshop mode, explores the new possibilities of distance teaching and team design cooperation in the future, and pays attention to integrating online and offline experiences. Learn about the participants' focus thresholds, the extension of the playbook, and communication methods. In terms of course organization, online courses can be divided into two types: massive open online Courses (MOOC) and miniature private online courses (SPOC), according to the openness of the organization and the scale of participation. Teaching methods such as live broadcasts, recorded broadcasts, online interaction, and digital resource sharing will be adopted. Most design project courses in colleges and universities embrace the SPOC model, which is convenient for real-time interaction between teachers and students and easy to ensure the quality of teaching. In addition, the software platform and hardware facilities used in the online course are also important factors that affect the course effect [10]. Online teaching promotes the innovation and reform of design courses, making learning professional theory and software skills more flexible and accessible. Compared with face-to-face classes, the English teaching project course based on network teaching is extensible, breaking through the limitations of time and space. Still, it is also limited by the physical environment, unable to use auxiliary objects, and has deficiencies in embodied cognition, separated from the experiment. In rooms and studios, some operational design work may need to be improved. In this environment, English teaching project courses face the challenges of insufficient practical conditions and environmental restrictions, and there is an urgent need for innovative teaching practices in terms of valuable forms, curriculum interaction, and design evaluation [15]. In the era of digital globalization, Online Education has become a cornerstone of learning, breaking down geographical barriers and fostering cross-cultural interactions. This paradigm shift necessitates a reevaluation of traditional teaching methods, especially in the context of teaching a global language such as English.

The English teaching project course is a vital teaching module for cultivating professional, comprehensive ability in English teaching students and adopts the project-based learning method. Based on the knowledge acquired in the introductory courses, students can master a complete set of design processes by completing specific practical projects and taking a problem-solving orientation. Based on the network teaching background, the English teaching project curriculum must use the network to expand the content and form. It is necessary to consider the design of theoretical methods to increase students' learning driving force and to design various practical approaches to lower the participation threshold to encourage students. Break through the screen limitations and actively participate in design practice [6].

The theme setting of the English teaching project curriculum needs to start with the fundamental interests and situations of students, consider the feasibility of practical operation, take into account social value and future exploration, guide students to pay attention to localized issues, and cultivate an international professional vision, and improve students' comprehensive design. And perception. The home learning venue and research conditions limit the online courses. Setting up localized design project course topics, making full use of existing resources as much as possible, allowing students to think about problems from their perspectives, and stimulating students' personalities according to their life situations, Interests, and initiatives [1]. The actual theme from the side and the local is convenient for design research and verification. At the same time, the theme should also consider the scalability of its direction and promote the production of various design solutions. Cultivate students' insight and empathy in localized design practice and shape designers with social responsibility [3].

Compared with theoretical courses, English teaching project courses pay more attention to design communication in practice and the construction of a reasonable design process, requiring

students to conduct design research around the project theme, construct plans, and verify the applicability of the plans. The English teaching project course based on network teaching should combine online theoretical guidance with offline design activities so that students can obtain a complete learning experience [16]. The online course design focuses on design theories and methods, design reviews and exchanges, and digital resource sharing. Offline courses focus on developing and summarizing students' autonomous situational exploration, design research, model-making, ergonomics, and other practical activities. The course sets staged tasks according to the project process. Students must complete purposeful design practice tasks after class and leave precious online time for design communication with professional tutors. Through the four links of learning, practice, communication, and reflection, alternately let students learn training, reflect in communication, and connect their offline and online learning and creative experiences [13].

Digitalization is the most significant feature of English teaching project courses based on network teaching. Digital learning resources and communication channels make disseminating and exchanging knowledge more convenient and provide a suitable learning experience. English teaching project courses should fully use network resources to expand the course content and network tools to organize and present innovations in design knowledge so that they conform to students' cognitive habits [11]. In the early stage of the course preparation, collect and sort out relevant network materials, edit the electronic documents required by the course, and help students understand the project theme and make preparations. Situational inquiry, problem definition, and scheme construction in the course also need students to consult a large amount of network information to make comprehensive judgments. The purpose is cultivating students' information retrieval and analysis abilities [12]. In network-based project teaching, digital communication is the most critical communication method. The interaction between teachers and students has replaced the previous face-to-face teaching with video, voice, graphics, and other forms of communication. At the same time, digital teaching increases the reproducibility of content. It is convenient for students to check for omissions and fill vacancies. When students report online, they can also communicate in the conference discussion area to learn about different design ideas and methods [2]. The design project report based on network teaching requires students' design processes and results to consider digital reading habits as much as possible to improve communication efficiency [14].

Design evaluation refers to the review of the output plan of the project and the learning effect of students in the English teaching project class. In the face-to-face English teaching project, students undergo a complete practical process. During the process, students can use many physical objects to corroborate their research findings and have abundant opportunities to go out to collect information. At the same time, they can use laboratory processing. Manufacture equipment to produce high-quality product models [9]. In the design evaluation of traditional English teaching project courses, the emphasis is on the performance of students' comprehensive design ability, and the project's final output occupies a large proportion of the design model effect. The primary consideration is the beauty and applicability of the model [5].

This paper combines artificial intelligence technology and a decision support system to improve the English online teaching mode and the intelligent level of English online teaching.

## **2 ALGORITHM RESEARCH AND OPTIMIZATION OF SURFACE SHAPE PERCEPTION SYSTEM**

### **2.1 Optical Path System of Distributed Online Teaching**

For fully distributed, high spatial resolution, and high-precision demodulation systems, demodulation systems using optical frequency domain reflection have higher advantages.

Therefore, an OFDR-based microcavity array fiber demodulation optical path is built, as shown in Figure 1. Since the system has strict requirements on the light source, Santec's TSL-710 narrow linewidth tunable laser is used as the light source in this paper, and its output parameter table is shown in Table 1.

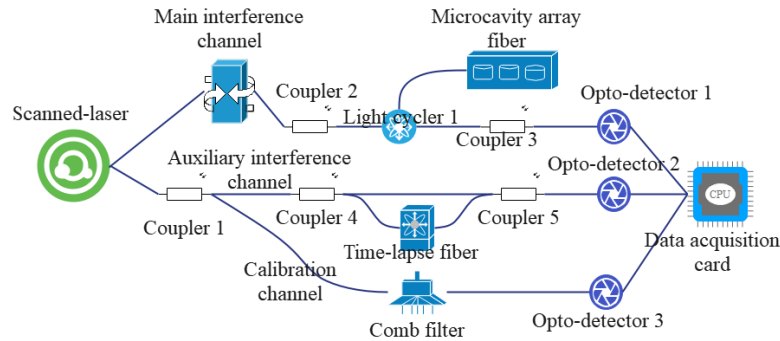


**Figure 1:** Fully distributed demodulation optical path.

The basic block diagram of microcavity array fiber demodulation based on optical frequency domain reflection is shown in Figure 2. It is assumed that the frequency of the light source output by the scanning laser changes linearly and that the light intensity remains constant. The light source is divided into two beams by the coupler C1 and enters the M-Z interferometer. Among them, the reference light that directly enters the coupler C2 through the C1 split beam is called the reference light, and the other beam is the signal light, which penetrates the microcavity array fiber through the circulator and is reflected by the microcavity unit. Then, it enters the coupler again through the circulator and interferes with the reference light to generate a high-frequency signal. After being converted into an electrical signal by a photoelectric converter, the microcavity unit's position and the reflection spectrum's demodulation are realized through frequency conversion.

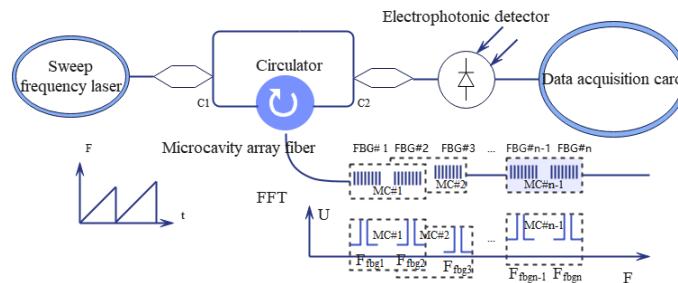


**Figure 2:** The principle of demodulation of the main interference channel.

### 1. Demodulation of microcavity array fiber position

Suppose it is assumed that the narrow linewidth light source output by the scanning laser is continuous light with a linearly changing frequency and constant light intensity. In that case, the optical signal output by the light source can be expressed as:

$$E(t_T, t) = E_0 \cos [2\pi(\nu_0 + \gamma_\nu t_T)t + \varphi_0] \quad (1)$$

If the fiber length from coupler 1 to coupler two is assumed to be  $L_N$ , the delay  $\tau_N$  of the reference optical signal passing through the signal arm to coupler C2 is:

$$\tau_N = \frac{L_N n_{eff}}{c} \quad (2)$$

In the formula,  $n_{eff}$  is the effective refractive index of the fiber, and  $c$  is the speed of light in vacuum. Therefore, the local oscillator light reaching coupler two can be expressed as:

$$E(t_T - \tau_1, t) = \eta E_0 \cos [2\pi(v_0 + \gamma_v(t_T - \tau_N))t + \varphi_0] \quad (3)$$

In the formula,  $\eta$  is a constant, which depends on the size of the splitting ratio. In the same way, the signal light entering the microcavity array fiber through the circulator and reflected to the coupler C2 can be expressed as:

$$E_{MC} = \Sigma E_0 \cos [2\pi(v_0 + \gamma_v(t_T - \tau_N))t + \varphi_0] \quad (4)$$

It represents the time delay from the reflected signal of the  $i$ -th grating in the microcavity array fiber to the coupler 2. If it is assumed that the distance from the  $i$ -th grating in the microcavity array fiber to the circulator is  $L$ , and the straight-line distance from coupler 1 to coupler 2 in the signal arm is  $LM$ , then  $\tau_i$  can be expressed as

$$\tau_i = \frac{(L_M + 2L_i)n_{eff}}{c} \quad (5)$$

Therefore, the intensity of the light field detected on the photodetector one is:

$$E_{PD} = E_{MC} + E(t_T - \tau_N, t) \quad (6)$$

Thus, the detected signal on the photodetector is expressed as:

$$u(t) = \frac{\{(E_1 + E_2) + \sigma E_0^2 \cos [2\pi(v_0 + \gamma_v(t_T - \tau_N))t + \varphi_0]\}}{\Sigma} \cdot \cos [2\pi(v_0 + \gamma_v(t_T - \tau_N))t + \varphi_0] \quad (7)$$

According to the product sum-difference formula, the above formula can be simplified to:

$$u(t) = \Sigma \left\{ (E_1 + E_2) + \frac{1}{2} \sigma E_0^2 \cos [2\pi(v_0 + \gamma_v(t_T - \tau_N))t + 2\varphi_0] + \frac{1}{2} \sigma E_0^2 \cos [2\pi(\gamma_v(\tau_i - \tau_N))t] \right\} \quad (8)$$

The above formula's optical frequency difference and the optical frequency sum term are obtained from the product and difference formula. However, due to the limited bandwidth of photodetectors, the optical frequency and term frequency reach the order of  $10^4$ . To sum up, the AC signal detected by the photodetector can be expressed as:

$$u(t) = \frac{1}{2} \sigma E_0^2 \Sigma \cos [2\pi(\gamma_v(t_T - \tau_N))t] \quad (9)$$

It can be known from formula (3-9) that the beat signal of each grating corresponds to a fixed frequency  $f_{bgt}$ .

$$f_{bgt} = \gamma_t(\tau_i - \tau_N) \quad (10)$$

Combining formula (5), the relationship between the position information of the grating and the frequency of the beat signal can be obtained as:

$$L_i = \frac{f_{bgt} \cdot c}{2\gamma_v n_{eff}} - \frac{L_M}{2} \quad (11)$$

It can be seen from the above formula that the position of the grating and the frequency of the beat signal correspond to each other.

According to the above analysis, it can be seen that the spatial resolution  $L$  of the demodulation system depends on the frequency resolution of the system and can be obtained by formula (11):

$$\Delta L = \frac{c}{2\gamma_v n_{eff} T} \quad (12)$$

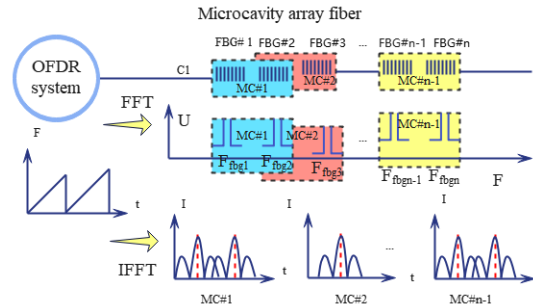


**Figure 3:** Spectral demodulation of microcavity unit.

The spectral demodulation process of the microcavity unit based on optical frequency domain reflection is shown in Figure 3. At the same time, acquiring the microcavity unit's reflection spectrum requires knowing each microcavity unit's beat frequency signal. According to the above analysis, in the microcavity array fiber, the beat signal of each grating can be separated in the frequency domain, and its frequency is proportional to the position of the grating. Therefore, the frequency range corresponding to MC#i can be selected using a sliding window filter, and then the inverse fast Fourier transform (IFFT) can be performed so that the beat frequency signal of MC#i can be separated from the aliased beat frequency-time domain signal.

The time corresponding to the central wavelength is  $t$ ; after sensing, the central wavelength is  $a$ , and the significant moment is  $t$ . Therefore, the change  $\Delta f$  of the output frequency of the laser can be obtained according to the time difference as:

$$\Delta f = \gamma_v \Delta t \quad (13)$$

The frequency of light can be represented by the wavelength and the speed of light so that  $\Delta f$  can be expressed as:

$$\Delta f = \frac{c}{\lambda_i} - \frac{c}{\lambda_r} = \frac{c(\lambda_r - \lambda_i)}{\lambda_i^2} \quad (14)$$

By substituting formula (13) into it, we can get:

$$\lambda_i = \lambda_r - \frac{\Delta t \gamma_v \lambda_r^2}{c} \quad (15)$$

Therefore, the wavelength resolution  $\Delta \lambda$  is:

$$\Delta \lambda = \frac{\gamma_v \lambda_r^2}{c f_s} \quad (16)$$

In the formula,  $f_s$  is the system's sampling rate set to 50MHz,  $\gamma_v = 12.5 * 10^{12}$ Hz/s. Therefore, the wavelength resolution of the system is  $\Delta\lambda \approx 0.002$  pm, and it can be seen that the system has a very high wavelength resolution.

## 2.2 High Spatial Resolution Demodulation Algorithm Optimization

The above analysis of the demodulation principle assumes that the optical frequency output by the light source changes linearly; that is,  $g$  is a constant. However, the light source used in the system changes linearly in wavelength, resulting in a nonlinear shift in the output frequency of the scanning light source. When  $\gamma_v$  is a constant, the beat frequency component of the grating is single, and when the light source has nonlinear effects, it will have problems such as spectral broadening. Hence, the nonlinear correction of the light source is significant.

When the frequency sweep speed is no longer constant,  $\gamma_v(t)$  can be regarded as a continuous  $\gamma_v$  and a change term. It results in that the phase of the beam output by the laser is no longer a constant  $\varphi_0$  but becomes a time-varying phase  $\varphi(t)$ . At this time, the laser output optical signal can be expressed as:

$$E(t_T, t) = E_0 \cos [2\pi(v_0 + \gamma_v t_T)t + \varphi_0] \quad (17)$$

At this time, the beat frequency signal received by the photodetector is:

$$u(t) = \frac{1}{2} \sigma E_0^2 \Sigma \cos [2\pi(\gamma_v(\tau_i - \tau_N))t + \varphi(t) - \varphi(t - (\tau_i - \tau_N))] \quad (18)$$

If  $\Delta\tau_i = \tau_i - \tau_N$ , the beat frequency of the grating can be obtained according to formula (10) as:

$$f_{\text{fbgt}} = \gamma_v(t)\Delta\tau = \gamma_v\Delta\tau + \frac{d(\varphi(t) - \varphi(t - \Delta\tau))}{2\pi dt} \quad (19)$$

In the above formula,  $\gamma_v(t)$  is the light source tuning speed.

To test the nonlinearity of this system, we used the optical path constructed above and tried it with the 'TSL-710 laser. The wavelength tuning speed is 100nm/s, the scanning range is 1540nm-1560nm, and the output optical power is 1mw. The end face reflection of the obtained measurement channel at 19.64m is shown in Figure 4. At this time, the end face reflection broadens by nearly 2.67m.

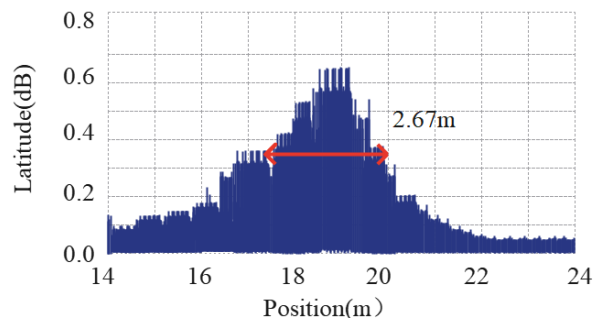


**Figure 4:** The reflection diagram of the end face of the measurement channel before nonlinear calibration.

If it is assumed that in the auxiliary interference channel, the arm length difference between the two paths is  $LM$ , the time difference  $\Delta\tau_{\text{cax}}$  of the beam reaching the coupler C2 is:

$$\Delta\tau_{aux} = \frac{LM^{neff}}{c} \quad (20)$$

According to formula (9), it can be deduced that the beat frequency signal detected by the photodetector is:

$$u_{aux} \propto E_0^2 \cos [2\pi\gamma_v \Delta\tau_{aux} t + \varphi(t) - \varphi(t - \Delta\tau_{aux})] \quad (21)$$

Since light propagates very fast in the fiber, it can be considered that  $\Delta\tau_{aux}$  is very small, and the following relationship exists at this time:

$$\varphi(t) - \varphi(t - \Delta\tau_{aux}) \approx \frac{d\varphi(t)}{dt} \Delta\tau_{aux} \quad (22)$$

Therefore, formula (21) can be simplified to:

$$u_{aux} \propto E_0^2 \cos \left( 2\pi\gamma_v \Delta\tau_{aux} t + \frac{d\varphi(t)}{dt} \Delta\tau_{aux} \right) \quad (23)$$

Similarly, in the main interference channel, the signal detected by the photodetector can be expressed as:

$$u(t) = \frac{1}{2} \sigma E_0^2 \Sigma \cos \left( 2\pi\gamma_v \Delta\tau_i t + \frac{d\varphi(t)}{dt} \Delta\tau_i \right) \quad (24)$$

In the formula,  $\Delta\tau_i = \tau_i - \tau_N$ . From formula (23) and formula (24), it can be concluded that the instantaneous phases of the main interference channel and the auxiliary interference channel satisfy the following relationship:

$$\varphi(t) \approx \frac{\Delta\tau_i}{\Delta\tau_{aux}} \varphi_{aux}(t) + \pi\gamma_v (\Delta\tau_{aux} - \Delta\tau_i) \quad (25)$$

It can be found from formula (25) that when both  $\Delta\tau_i$  and  $\Delta\tau_{aux}$  are very small, it can be approximately considered that the time corresponding to the phase interval of the beat signal of the auxiliary interference channel and the time related to the phase interval of the beat signal of the main interference channel are equal.

In this paper, the Hilbert transform is used to obtain the phase of the auxiliary interference channel. The Hilbert transform of the additional channel signal can be obtained:

$$H(u_{aux}) = E_0^2 \sin \left( 2\pi\gamma_v \Delta\tau_{aux} t + \frac{d\varphi(t)}{dt} \Delta\tau_{aux} \right) \quad (26)$$

Therefore, the instantaneous phase of the light source can be expressed as:

$$\varphi(t) = \arctan (H(u_{aux})/u_{aux}) \quad (27)$$

In this paper, the process of nonlinear calibration is shown in Figure 6, and the specific process is as shown in the figure.

As shown in Figure 7, the spatial resolution of the original flattened signal is broadened to 2.67m. After nonlinear calibration, the spatial resolution is improved to 80.25um.

To reduce the influence of the light source tuning speed on the demodulation system, this paper uses the scanning speed obtained in the light source nonlinear compensation algorithm as the actual tuning speed of the light source. It uses the generated equal-phase interval to calculate the scanning speed of the light source.

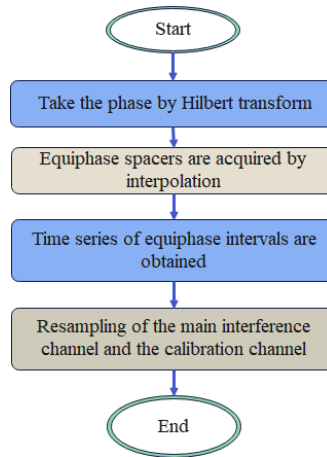


**Figure 6:** Flow chart of nonlinear calibration.

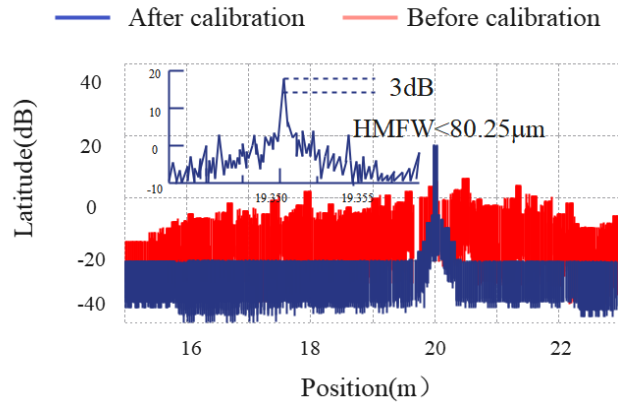


**Figure 7:** Spectrogram of the main interference channel after nonlinear calibration.

According to the phase information of the auxiliary interference channel in formula (23), the scanning speed after nonlinear compensation can be obtained and can be expressed as:

$$\gamma_{v-act} = \frac{\varphi_{aux}(T)}{2\pi\Delta\tau_{aux}T} \quad (28)$$

In the formula,  $T$  represents the sampling time, and  $\varphi_{aux}(T)$  is the phase value of the beat signal of the auxiliary interference channel at time  $T$ .

### 2.3 Surface Shape Perception Algorithm Based on Curvature Information

As shown in Figure 11, we assume that the micro-element  $AB$  coincides with the  $X$ -axis before bending and establish the primary coordinate system  $XY$  based on this. Moreover, we believe it becomes an arc shape, as shown in the figure, after turning and setting  $X'Y'$  with the tangent direction of the starting position  $A$  of the micro-element as the axis of the  $x'$  secondary coordinate system. The coordinate of the end point  $B$  of the micro-element  $AB$  in the coordinate system  $XY$  is

$(x_B, y_B)$ ; that is, the projections of point B on the X-axis and the Y-axis are  $x_B$  and  $y_B$ , respectively. The coordinate of B in the coordinate system X'Y' is  $(x'_B, y'_B)$ , that is, the projections of point B on the X' axis and the Y' axis are  $x'_B$  and  $y'_B$ , respectively. The projection point of point B on the X' axis in the coordinate system X'Y' is B', the coordinate of point B' in the coordinate system XY is  $(x_{B1}, y_{B1})$ , and the radius of curvature of the micro-element AB is  $\rho_{AB}$ , the central angle is  $\alpha$ . The angle between the tangent of the starting point A and the X-axis is  $\theta$ . According to the differential geometry of microelements, the angle  $\theta$  between the tangent of the starting point A and the X axis can be expressed as:

$$\theta = \int_0^s k(s)ds \quad (29)$$

In the coordinate system XY, there is the following relationship:

$$\begin{cases} x_B = x_{B1} - \Delta = x'_B \cdot \cos \theta - \Delta \\ y_B = y_{B1} + \tau = x'_B \cdot \sin \theta + \tau \end{cases} \quad (30)$$

In the formula,  $\tau$  represents the distance between the projection points  $y_B$  and  $y_{B1}$ ,  $\Delta$  represents the distance between the projection points  $x_B$  and  $x_{B1}$ , and satisfies the following relationship:

$$\begin{cases} \Delta = y'_B \cdot \sin \theta \\ \tau = y'_B \cdot \cos \theta \end{cases} \quad (31)$$

By substituting formula (32) into equation (31), we get:

$$\begin{cases} x_B = x'_B \cdot \cos \theta - y'_B \cdot \sin \theta \\ y_B = x'_B \cdot \sin \theta + y'_B \cdot \cos \theta \end{cases} \quad (32)$$

Similarly, in the coordinate system X' Y',

$$\begin{cases} x'_B = \rho_{AB} \cdot \sin \alpha \\ y'_B = \rho_{AB} - \rho_{AB} \cdot \cos \alpha \end{cases} \quad (33)$$

For the micro-element AB, the reciprocal of its curvature can be represented by the inverse of the curvature of the starting point  $\Delta$  and the ending point B:

$$\frac{1}{k_{AB}} = \rho_{AB} = \frac{k_A + k_B}{2k_A \cdot k_B} \quad (34)$$

Moreover, from the arc length formula, we can get:

$$s = \alpha \cdot \rho_{AB} \quad (35)$$

In the formula, s represents the arc length of the micro-element AB,  $k_A$  represents the curvature of the starting point  $\Delta$ , and k represents the curvature of the endpoint B. By substituting formula (34) and formula (35) into formula (33), respectively, we can get:

$$\begin{cases} x'_B = \frac{k_A + k_B}{2k_A \cdot k_B} \cdot \sin \frac{s}{\rho_{AB}} = \frac{k_A + k_B}{2k_A \cdot k_B} \cdot \sin \frac{s(2k_A \cdot k_B)}{k_A + k_B} \\ y'_B = \frac{k_A + k_B}{2k_A \cdot k_B} \cdot (1 - \cos \alpha) = \frac{k_A + k_B}{2k_A \cdot k_B} \cdot \left(1 - \cos \frac{s(2k_A \cdot k_B)}{k_A + k_B}\right) \end{cases} \quad (36)$$

According to formulas (32) and (36), the coordinate increment  $(x_B, y_B)$  of point B in the micro-element AB can be obtained. On this basis, the coordinate increment of the end point coordinate of each segment relative to the starting point is obtained, and the cycle is repeated until all the coordinates of the microelement segment of the entire curve are solved.

### 3 ONLINE ENGLISH TEACHING MODE BASED ON ARTIFICIAL INTELLIGENCE TECHNOLOGY AND DECISION SUPPORT SYSTEM

To adapt to the characteristics of college teaching decision-making needs, we designed a structured three-layer college English online teaching decision support system architecture, as shown in Figure 8.

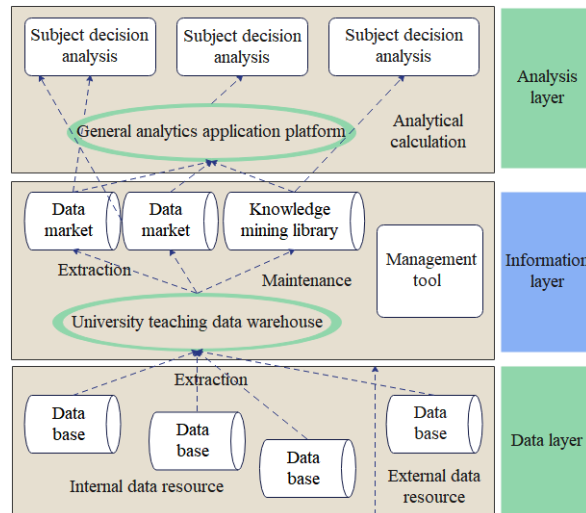
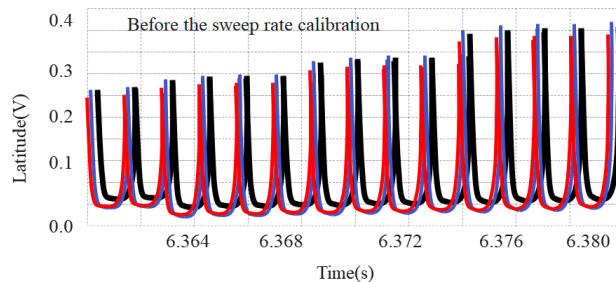


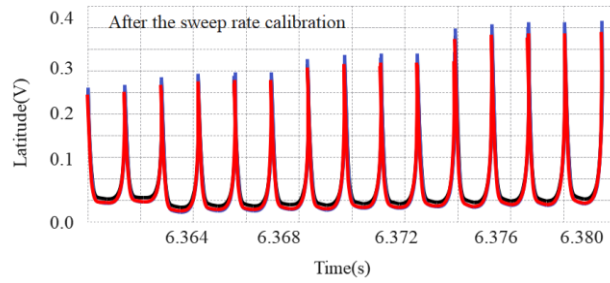
**Figure 8:** Architecture of college English online teaching decision support system.

In this paper, the algorithm of the second part is applied to the feature recognition of English teaching and combined with the decision-making system shown in Figure 8 to improve the online English teaching mode.

In this paper, the scanning speed calculated by equation (28) is substituted into equation (11) to obtain the distance domain information of the compensated microcavity array fiber. Moreover, this paper compares it with the information in the distance domain before calibration, selects the same microcavity array fiber, performs multiple measurements, and restores the spectral data in the distance domain. The light source scanning range is 1540nm-1560nm, the scanning speed is 100nm/s, the sampling rate is 50MHz, and the sampling time is 0.2s. The results are shown in Figure 8. Figure (a) is the spectrum of the microcavity array fiber in the distance domain of 6.36m-6.38m before calibration. It can be found that when the scanning speed calibration is not performed, the microcavity array fiber is jittered left and right in the distance domain. Figure (b) is the distance domain spectrogram of the microcavity array fiber after scanning speed calibration. At this point, the gratings in the microcavity array fiber are entirely overlapped.



(a) Before the sweep rate calibration spectrum map



(b) After sweep rate calibration spectrum map

**Figure 9:** Spectrogram of the main interference channel before and after scanning speed calibration.

## 2. Wavelength axis calibration

To ensure that during the repeated sampling process of the system, each sampling point is in the same wavelength range, in this paper, a calibration channel is added to the optical path to calibrate the wavelength axis. The channel mainly comprises a comb filter calibrated by its thermal stability and comb peaks with equal intervals. The transmission peak detected by the photodetector is shown in Figure 3-9.

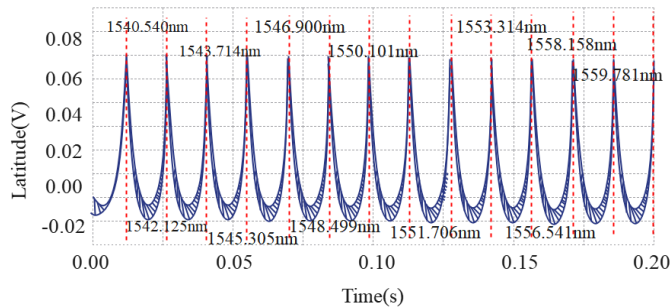


**Figure 10:** Transmission peak of the comb filter.

As the above figure shows, the comb filter's transmission spectrum consists of multiple single peaks, and the wavelength value corresponding to each single peak can be measured by calibration. Therefore, the wavelength value corresponding to each moment on the entire time axis can be calculated with the wavelength scanning speed calibrated above to complete the conversion of the wavelength axis and the time axis, thereby realizing the calibration of the wavelength axis. It can be obtained that the wavelength values corresponding to each time point after calibration are:

$$\lambda_i = \frac{1}{N} \sum_{n=1}^N \frac{c}{f_n - \gamma_{v-act}(t_i - t_n)} \quad (37)$$

In the formula,  $N$  represents the number of single peaks in the transmission peak of the comb filter within the sampling time. In this paper, the sampling time is 0.2s, the wavelength scanning range is 1540nm-1560nm, and the frequency interval of the comb filter is 50GHz. Therefore, the number of single peaks obtained by sampling is 12,  $t_n$  represents the time corresponding to the  $n$ -th single peak, and  $f_n$  represents the optical frequency corresponding to the  $n$ th single peak, which

can be obtained by using the calibrated wavelength,  $t_i$  represents the sampling time, and  $\gamma_t$  represents the wavelength value corresponding to the calibrated sampling time  $t_i$ .

To improve the calibration accuracy, this paper first performs Gaussian fitting on the transmission peaks output by the comb filter and accurately calculates the time corresponding to each peak. Then, this paper uses each peak to find and average the wavelength axis to improve the calibration accuracy.

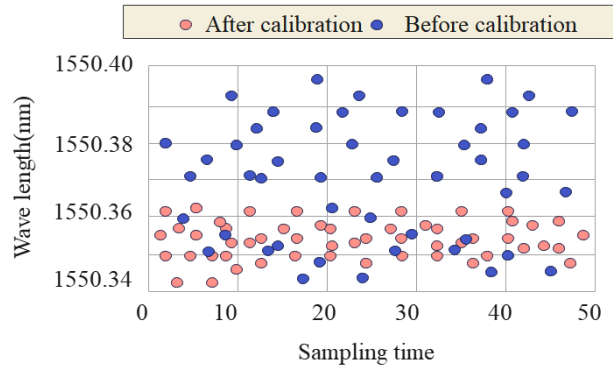


**Figure 11:** Comparison diagram before and after wavelength calibration.

To verify the demodulation effect after wavelength calibration, this paper conducts a comparison through experiments. Moreover, in this paper, the microcavity unit at the end of the microcavity array fiber with a grating length of 0.5mm, an interval of 0.5mm, a reflectivity of -45dB, and a total length of 7.9m is selected for demodulation. In this paper, 50 sets of data are continuously collected in a stable environment and demodulated before and after the calibration of the wavelength axis, respectively. The results obtained are shown in Figure 10. Before calibration, the wavelength jitter range reached 56pm, and after calibration, the wavelength jitter range was 11 pm. It can be found that, after wavelength calibration, the jitter of the demodulation wavelength is improved, and the precision of the demodulation system is greatly improved.

Based on the above analysis, the teaching effect of the online English teaching mode based on artificial intelligence technology and the decision support system proposed in this paper is verified, and Table 1 is obtained.

<i>Num</i>	<i>Teaching verification</i>	<i>Num</i>	<i>Teaching verification</i>	<i>Num</i>	<i>Teaching verification</i>
1	87.990	14	87.096	27	85.332
2	86.590	15	87.199	28	87.150
3	86.905	16	86.855	29	83.974
4	87.265	17	83.852	30	83.916
5	85.641	18	84.088	31	83.067
6	83.773	19	86.425	32	87.461
7	86.529	20	87.954	33	83.523
8	87.259	21	87.855	34	86.354
9	83.297	22	86.613	35	86.063
10	84.611	23	86.542	36	87.653

11	84.778	24	86.693	37	83.832
12	87.604	25	86.771	38	83.615
13	86.001	26	87.629	39	86.700

**Table 1:** Teaching system effect verification.

From the above research, the online English teaching model based on artificial intelligence technology and the decision support system proposed in this paper can effectively improve the effect of online English teaching.

#### 4 CONCLUSIONS

Network-based synchronous online teaching has been used as auxiliary teaching in the early days. After that, due to the increase in user demand, the advancement of information technology, and policy support, it began to develop rapidly. In early 2020, affected by the new crown epidemic, the world experienced the most extensive online education practice in history. At the same time, many designs professional courses have also begun to explore the network teaching mode. Combined with online teaching, the teaching reform of the course on environmental design performance techniques is carried out, and the rich resources and communication methods of online teaching are fully utilized to help students learn performance techniques. This paper combines artificial intelligence technology and a decision support system to improve the English online teaching mode and the intelligent level of English online teaching. The research shows that the online English teaching mode based on artificial intelligence technology and the decision support system proposed in this paper can effectively improve the effect of online English teaching.

Jing Chen, <https://orcid.org/0009-0005-0563-7486>

Jindan Yang, <https://orcid.org/0009-0001-7274-6448>

#### REFERENCES

- [1] Abdelshaheed, B. S.: Using Flipped Learning Model in Teaching English Language among Female English Majors in Majmaah University, *English Language Teaching*, 10(11), 2017, 96-110. <https://doi.org/10.5539/elt.v10n11p96>
- [2] Agung, A. S. N.: Current Challenges in Teaching English in Least-developed Region in Indonesia. *SOSHUM: Jurnal Sosial Dan Humaniora*, 9(3), 2019, 266-271. <https://doi.org/10.31940/soshum.v9i3.1317>
- [3] Ashraf, T. A.: Teaching English as a Foreign Language in Saudi Arabia: Struggles and Strategies, *International Journal of English Language Education*, 6(1), 2018, 133-154. <https://doi.org/10.5296/ijelev.v6i1.13148>
- [4] Ayçiçek, B.; YanparYelken, T.: The Effect of Flipped Classroom Model on Students' Classroom Engagement in Teaching English, *International Journal of Instruction*, 11(2), 2018, 385-398. <https://doi.org/10.12973/iji.2018.11226a>
- [5] Coşkun, A.: The Application of Lesson Study in Teaching English as a Foreign Language, *Inonu University Journal of the Faculty of Education*, 18(1), 2017, 151-162. <https://doi.org/10.17679/inuefd.297845>
- [6] Gupta, A.: Principles and Practices of Teaching English Language Learners, *International Education Studies*, 12(7), 2019, 49-57. <https://doi.org/10.5539/ies.v12n7p49>
- [7] Guzachchova, N.: Zoom Technology as an Effective Tool for Distance Learning in Teaching English to Medical Students, *Bulletin of Science and Practice*, 6(5), 2020, 457-460. <https://doi.org/10.33619/2414-2948/54/61>

- [8] Hadi, M. S.: The Use of Song in Teaching English for Junior High School Student, *English Language in Focus*, 1(2), 2019, 107-112. <https://doi.org/10.24853/elif.1.2.107-112>
- [9] Kelly, L. B. Preservice Teachers' Developing Conceptions of Teaching English Learners, *Tesol Quarterly*, 52(1), 2018, 110-136. <https://doi.org/10.1002/tesq.375>
- [10] Mahboob, A.: Beyond global Englishes: Teaching English as a Dynamic Language, *RELC Journal*, 49(1), 2018, 36-57. <https://doi.org/10.1177/0033688218754944>
- [11] Nurhayati, D. A. W.: Students' Perspective on Innovative Teaching Model Using Edmodo in Teaching English Phonology: " A Virtual Class Development." *DinamikaIlmu*, 19(1), 2019, 13-35. <https://doi.org/10.21093/di.v19i1.1379>
- [12] Rinekso, A. B.; Muslim, A. B.: Synchronous Online Discussion: Teaching English in higher Education Amidst the Covid-19 Pandemic, *JEEES (Journal of English Educators Society)*, 5(2), 2020, 155-162. <https://doi.org/10.21070/jees.v5i2.646>
- [13] Sayakhan, N. I.; Bradley, D. H.: A Nursery Rhymes as a Vehicle for Teaching English as a Foreign Language, *Journal of University of Raparin*, 6(1), 2019, 44-55. [https://doi.org/10.26750/vol\(6\).no\(1\).paper4](https://doi.org/10.26750/vol(6).no(1).paper4)
- [14] Saydaliyeva, M. A.; Atamirzayeva, E. B.; Dadaboyeva, F. X.: Modern Methods of Teaching English in Namangan State University, *International Journal on Integrated Education*, 3(1), 2020, 8-9. <https://doi.org/10.31149/ijie.v3i1.256>
- [15] Sundari, H. Classroom Interaction in Teaching English as Foreign Language at Lower Secondary Schools in Indonesia, *Advances in Language and Literary Studies*, 8(6), 2017, 147-154. <https://doi.org/10.7575/aiac.all.v.8n.6p.147>
- [16] Tarnopolsky, O.: Principled Pragmatism, or Well-Grounded Eclecticism: A New Paradigm in Teaching English as a Foreign Language at Ukrainian Tertiary Schools? *Advanced Education*, (10), 2018, 5-11. <https://doi.org/10.20535/2410-8286.133270>